

# Integrated Ugi-Based Assembly of Functional, Skeletal and Stereochemically Diverse 1,4-Benzodiazepin-2-ones

Jhonny Azuaje,<sup>1,2</sup> José M. Pérez-Rubio,<sup>1,2</sup> Vicente Yaziji,<sup>1,2</sup> Abdelaziz El Maatougui,<sup>1,2</sup> José Carlos González-Gomez,<sup>3</sup> Víctor Sánchez-Pedregal,<sup>1</sup> Armando Navarro-Vázquez,<sup>4</sup> Christian F. Masaguer<sup>2</sup> Marta Teijeira,<sup>4</sup> and Eddy Sotelo<sup>1,2\*</sup>

<sup>1</sup>Centro Singular de Investigación en Química Biológica y Materiales Moleculares (CIQUS) and <sup>2</sup>Departamento de Química Orgánica, Facultad de Farmacia.

Universidad de Santiago de Compostela. E-15782. Santiago de Compostela (Spain).

<sup>3</sup>Instituto de Síntesis Orgánica, Facultad de Ciencias. Universidad de Alicante. E-03080-Alicante (Spain). <sup>4</sup>Departamento de Química Orgánica, Facultad de

Química. Universidad de Vigo. E-36310-Vigo (Spain).

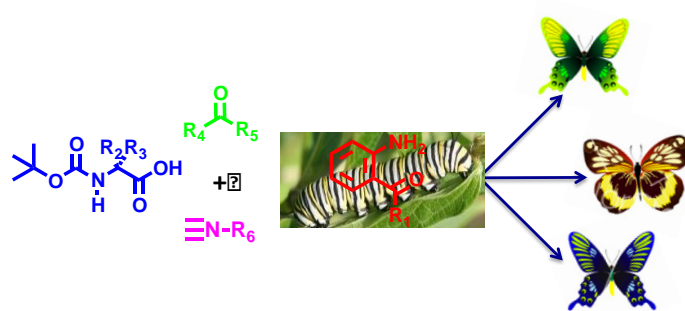
**Key words:** Benzodiazepines, Ugi Reaction, Isocyanides, Multicomponent Reaction.

**Abstract:** A practical, integrated and versatile U-4CR-based assembly of 1,4-benzodiazepin-2-ones exhibiting functional, skeletal and stereochemically diverse substitution patterns is described. By virtue of its convergence, atom economy and bond-forming efficiency herein documented methodology exemplify the reconciliation of structural complexity and experimental simplicity in the context of medicinal chemistry projects.

\*Corresponding author: Prof. Eddy Sotelo.

tel.: ++34-881-815732, Fax.: ++34-981-528093, e-mail: e.sotelo@usc.es

**Graphical Abstract:**



## Introduction

Extensively employed as therapeutics since the early 1960s 1,4-benzodiazepin-2-ones (BZDs) embody the archetypical privileged structure,<sup>1</sup> a concept coined by Evans in the late 1980s<sup>2</sup> and that constitute a fruitful strategy to improve the low hit rates usually experienced during high-throughput screening campaigns. Whereas BZD scaffolds are recurrent templates in the context of CNS therapies (being extensively prescribed as sedatives, anxiolytics, anticonvulsants or muscle relaxants),<sup>3</sup> the continuous appearance of reports describing novel pharmacological activities (e.g. antitumor, anti-HIV, antiarrhythmic, antitrypanosomal)<sup>4</sup> unequivocally corroborate the ability of BZDs to modulate biological targets beyond CNS targets (Figure 1).

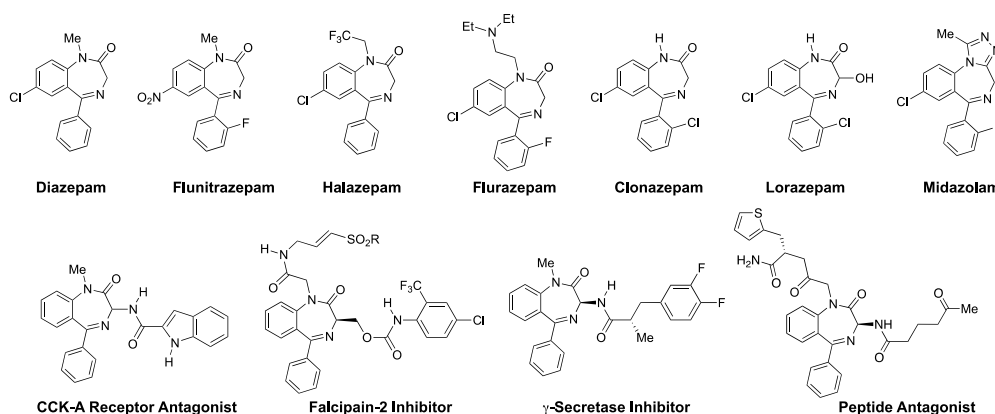


**Figure 1.** Representative drugs and bioactive compounds derived from the 1,4-benzodiazepin-2-one scaffold.

The BZD's pharmacogenicity profile heavily relies on its constrained peptide mimic nature,<sup>3,4</sup> which dictates the geometry of the heterocyclic core and its appended functional groups, thus modulating the structural parameters ultimately governing ligand/receptor interactions. In such a context it should be emphasized that BZDs exist in a boat conformation, which confers intrinsic chirality to the heterocyclic core even in the absence of stereogenic carbons.<sup>5</sup> The barrier for racemization between (*M*)- and (*P*)-

enantiomers is known to be low,<sup>5,6</sup> unless they exhibit a single substituent at C3 -which is stabilized at the pseudoequatorial position- or a relatively large substituent at position 1.<sup>7</sup> Consequently, the stereochemical diversity in BZD's collections can be easily expanded by combining the chirality of the heterocyclic core with stereocenters at C3 or by introduction of chiral side-chains at position 1 of the framework.

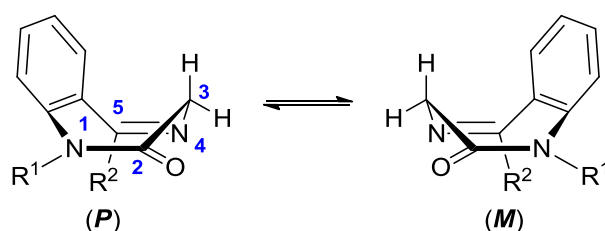


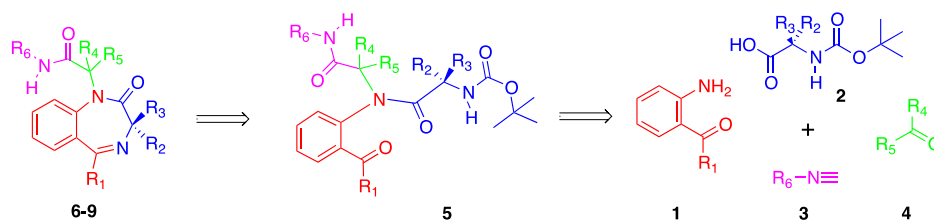
**Figure 2.** (*P*) and (*M*) conformational enantiomers of 1,4-benzodiazepin-2-ones.

In addition to the bioactivity issues, the versatility of a privileged scaffold is heavily dependent on two key factors: its synthetic feasibility and its ability to be decorated and/or reinterpreted according to the specific requirements of distinct biological targets. Therefore, the implementation of concise and efficient synthetic methodologies providing integrated access to privileged molecular frameworks eliciting functional, skeletal as well as stereochemical diversity, while enabling the reconciliation of the molecular complexity with experimental simplicity, constitutes a highly appreciated goal within the competitive environment of drug discovery. Despite the plethora of synthetic methods targeting BZDs,<sup>8</sup> established approaches consist in multistep linear pathways; where diversity elements are usually early introduced. Epimerization is often an issue; particularly during the subsequent functionalization stages of the heterocycle.<sup>9</sup> A valuable incorporation to the compendium of preparative methods targeting BZDs includes multicomponent reactions (MCR);<sup>10</sup> which have emerged as a tailored synthetic paradigm in drug discovery. Perhaps the most powerful MCR-assisted method

for generating BZD libraries<sup>11</sup> involves the Ugi four-component reaction (U-4CR).<sup>12</sup> Whereas this strategy has provided examples of elegant access to diverse BZD scaffolds,<sup>11,12</sup> most described protocols still require several synthetic steps and/or structurally elaborate precursors; thereby hampering its extensive application in medicinal chemistry programs. Additionally, the development of modular MCR-based approaches providing collections of privileged molecular frameworks in enantio- or diastereo- pure fashion remains a highly elusive challenge.<sup>11</sup> We herein document a conceptually simple and modular U-4CR-based approach that provides an integrated access to functional, skeletal and stereochemically diverse chemotypes derived of the pharmacologically useful 1,4-benzodiazepin-2-one framework.

## Results and Discussion

In the frame of a medicinal chemistry program series of 1,4-benzodiazepin-2-ones, simultaneously incorporating functionalized alkyl chains at N1 and concise chemical and stereochemical substitution patterns at position 3 of the heterocyclic core, were required. Being aware of the limitations of classical synthetic approaches to access the targeted chemotypes, we decided to assess the feasibility of a MCR-based approach. It was envisioned (Scheme 1) that the U-4CR reaction employing 2-aminophenylketones (**1**) as amine input, in combination with *N*-Boc protected aminoacids (**2**), isocyanides (**3**) and a carbonyl partner (**4**), would afford the corresponding Ugi adducts (**5**), which upon removal of the protecting group would undergo an intramolecular cyclization to provide the targeted BZDs (Scheme 1). The feasibility of the proposed approach relies heavily on the reactivity of the carbonyl moiety of the starting 2-aminophenylketone (**1**) when coexisting with alternative carbonyl compounds during the U-4CR.



**Scheme 1.** Retrosynthetic analysis to BZD derivatives **6–9** through U-4CR.

While a few reports have exemplified the use of aminoketones (**1**) toward U-4CR,<sup>13</sup> to the best of our knowledge, these works have employed aldehydes as carbonyl components; remaining unexplored the reaction outcome of this transformation with ketones. Two recent papers have described Ugi-based benzodiazepine synthesis conceptually related to herein document approach. The first study, published by Torroba et al. in 2010,<sup>14</sup> documents an U-4CR that employs 2-aminobenzophenone and (S)-2-azido-3-phenylpropanoic acid as key components (in combination with cyclohexylisocyanide and three substituted benzaldehydes); thus generating Ugi adducts that were subsequently cyclized under the Staudinger/aza-Wittig reaction conditions. This elegant approach is, notwithstanding, strongly limited by the scarce availability of functional and stereochemical diverse 2-azidopropanoic acids. This paper inspired the design of the herein documented pathway (Scheme 1). As observed, it follows the Ugi-deprotect-Cyclize (UDC) strategy and capitalizes the availability functional and stereochemical diversity of N-Boc protected aminoacids (**2**). During the practical implementation of our study a communication<sup>15</sup> described several novel U-4CR approaches to 1,4-benzodiazepine scaffolds; one of them briefly exploring herein documented approach. Since our exhaustive examination of the transformation reveals novel reactivity facets and expand method's scope, but also provides novel 1,4-benzodiazepin-2-ones chemotypes featuring unexplored functional, skeletal and stereochemical substitution patterns (Figure 2), we decided to present our results.

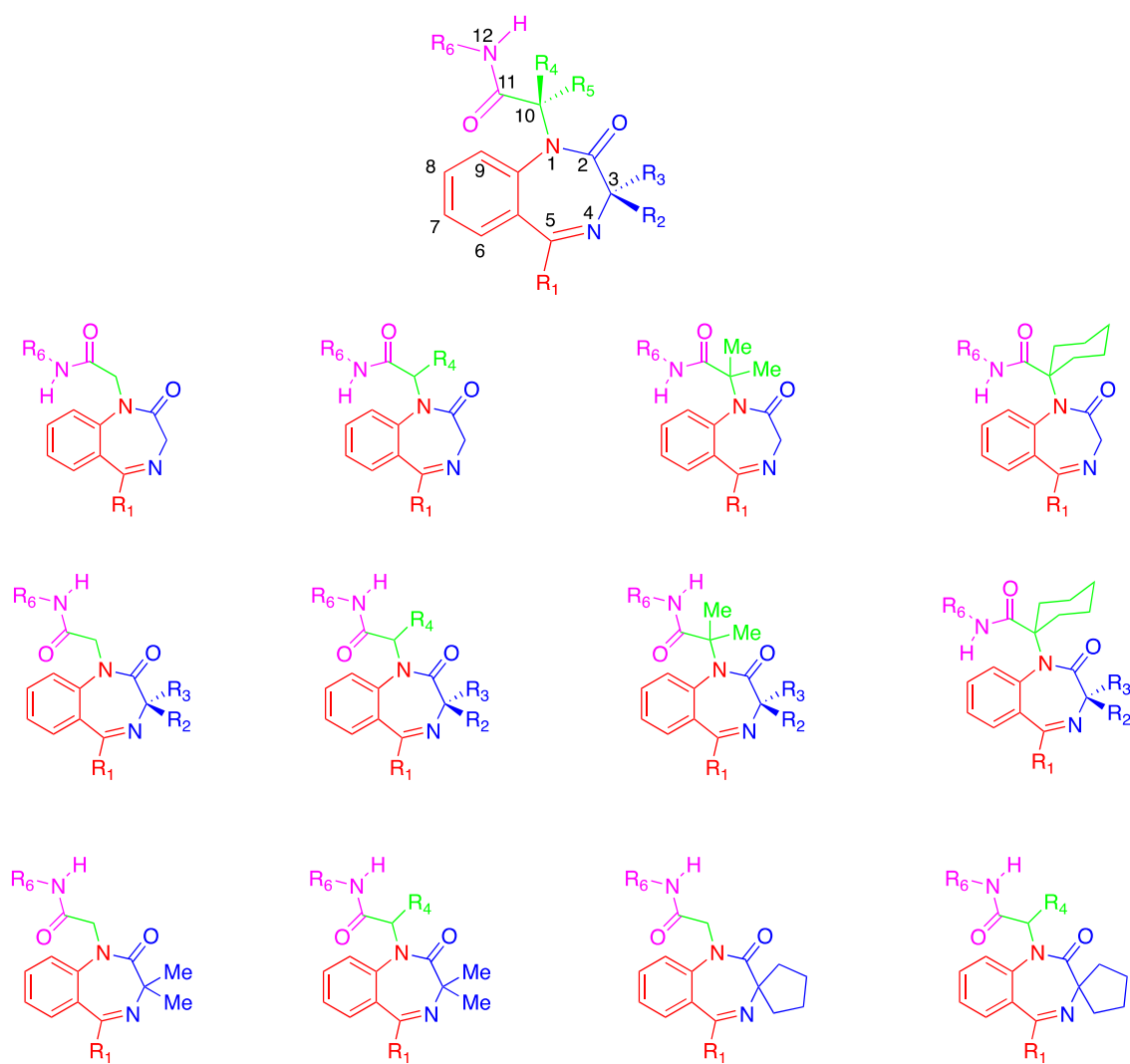
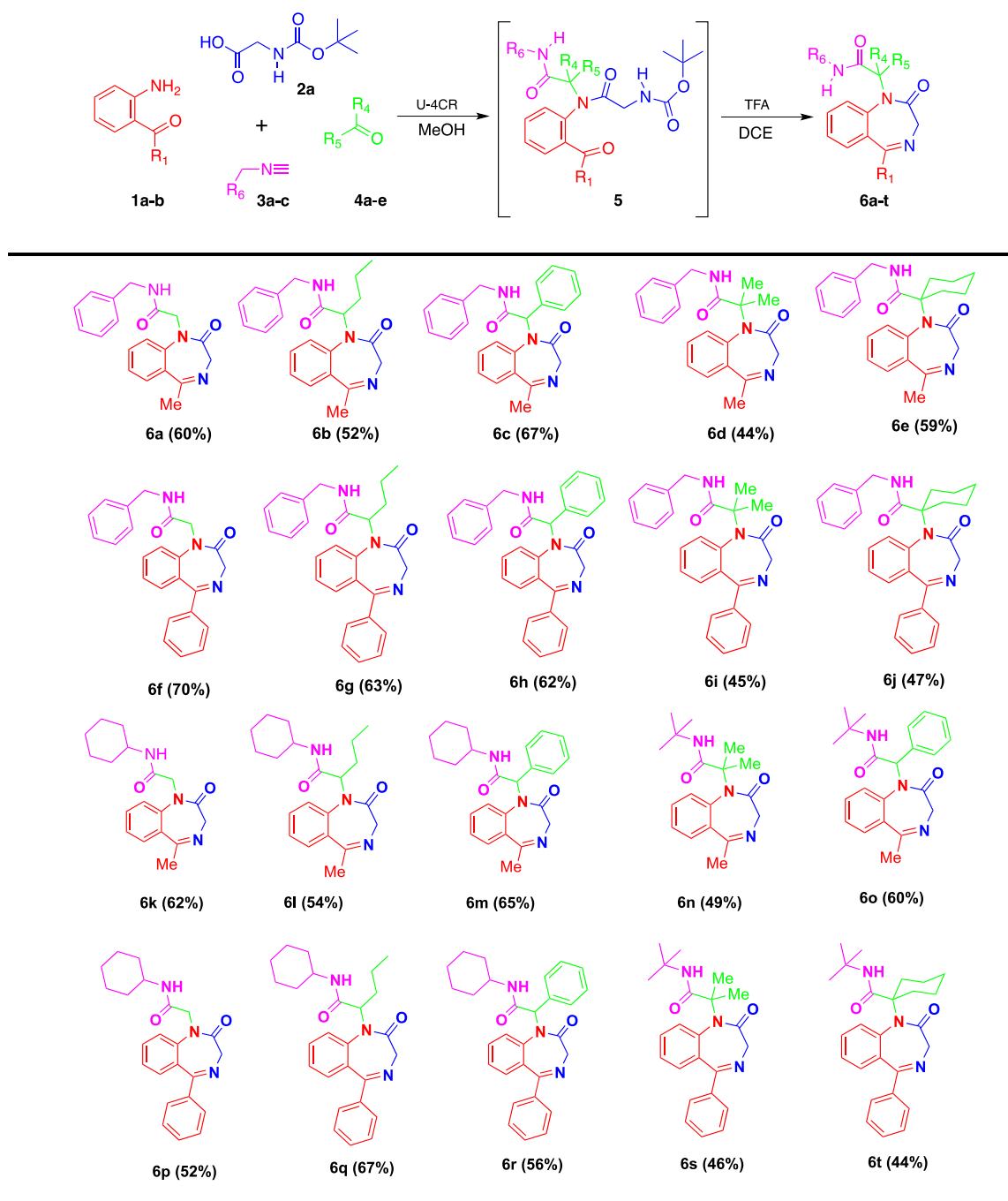


**Figure 3.** Structure and numbering of 1,4-benzodiazepin-2-one chemotypes (**6-9**) assembled through the Ugi-based approach herein described.

As a proof of concept (Scheme 2) 2-aminobenzophenone (**1a**) and 2-aminoacetophenone (**1b**) were selected as model amine substrates for the Ugi reaction, in combination with glycine Boc (**2a**) and benzyl isocyanide (**3a**). With the aim to exhaustively evaluate the chemoselectivity profile of the transformation, and consequentially its robustness and potential contribution in terms of chemical diversity, aldehydes [e.g. formaldehyde (**4a**), butyraldehyde (**4b**) and benzaldehyde (**4c**)] but also ketones [e.g. propanone (**4d**) and cyclohexanone (**4e**)] were employed as reactive inputs (Scheme 2). The selected substrates were submitted to the standard conditions of the Ugi condensation in methanol (Scheme 2). Analysis of reaction behaviour for model substrates revealed that transformations are successful regardless of the steric hindering present at either the amine (**1**) or the carbonylic partners (**4**); with more than 85% of **1** consumed after 36 h in most experiments (independently of the use of aldehyde or ketone). The intermediacy of the  $\alpha$ -acylamino amides **5** was unequivocally confirmed by the spectroscopic methods. It was gratifying to find that, upon reaction quenching and subsequent cleavage of the protecting group, Ugi adducts are readily transformed; triggering BZDs **6** in a two-step one-pot fashion with overall yields ranging 46-77% (Scheme 2). Among a variety of tested reagents to remove the BOC group, 20% TFA in DCE at 60°C provided an efficient cleavage while simultaneously promoting mild cyclization in short reaction times (0.5-1 h). With the aim to evaluate the robustness of the method, the reactivity of other isocyanides [e.g. cyclohexyl (**3b**) or tert-butyl (**3c**)] was preliminarily tested; thus generating the 1,4-benzodiazepin-2-ones **6k-t**. In concordance with previous observations,<sup>16</sup> the use of polystyrene supported *p*-toluenesulfonic acid once finished the U-4CR, in addition to remove traces of the remaining isocyanide, simultaneously scavenges the unreacted amine (**1**); thus simplifying the purification stage.



## Scheme 2. Ugi-Based Assembly of 1,4-benzodiazepin-2-ones **6**.



As observed (Scheme 2), both aldehydes (aliphatic or aromatic) and ketones (acyclic and cyclic) were found to be good substrates, with the transformation exhibiting complete chemoselectivity. It should be highlighted that the herein documented strategy enables the straightforward introduction of challenging residues on

the exocyclic acetamide linkage under neutral conditions, as represented for 2,2-dimethyl derivatives (**6d**, **6i**, **6n** and **6s**) and particularly for the cyclohexyl analogues (**6e**, **6j** and **6t**). In addition to validate the feasibility of the proposed pathway, the results included in scheme 2 provide a preliminary assessment of the exploratory power of this conceptual and experimentally simple strategy. It should be noticed that herein documented strategy assemble BZDs **6** in a one-pot procedure that involves the formation of six new bonds; thus exhibiting outstanding bond-forming efficiency and step economy.

Analysis of the NMR spectra of compounds **6a-t** enables to observe that exchange between the two boat enantiomeric conformations P and M is slow in the NMR chemical shift time scale, as previously observed for BZDs with bulky substituents on N1.<sup>7</sup> This is assessed by observing the C3 protons resonances in the <sup>1</sup>H-NMR spectrum. At room temperature the H3 protons are observed as two well separated doublets ( $\delta$  H<sub>ax</sub> ~3.5 ppm vs.  $\delta$  H<sub>eq</sub> ~4.5 ppm,  $|^2J_{\text{HH}}| = 10.5 - 12.5$  Hz). The strong shielding of the pseudoaxial proton H<sub>ax</sub> is caused by the phenyl ring of the BZDs skeleton. When prochiral aldehydes were used in the Ugi reaction (e.g. **4b** and **4c**) a new stereocenter is introduced in the side chain at position 1' and the (P) and (M) boat conformations become diastereomeric (Figure 4). In the <sup>1</sup>H-NMR spectra of these compounds (**6b**, **6c**, **6g**, **6h**, **6l**, **6m**, **6o**, **6q**, **6r**), resonances corresponding to each diastereomeric pair of enantiomers —(*P,S*)/(*M,R*) vs (*P,R*)/(*M,S*)— can be seen, with diastereomeric ratios ranging from 1:2 to 1:5.

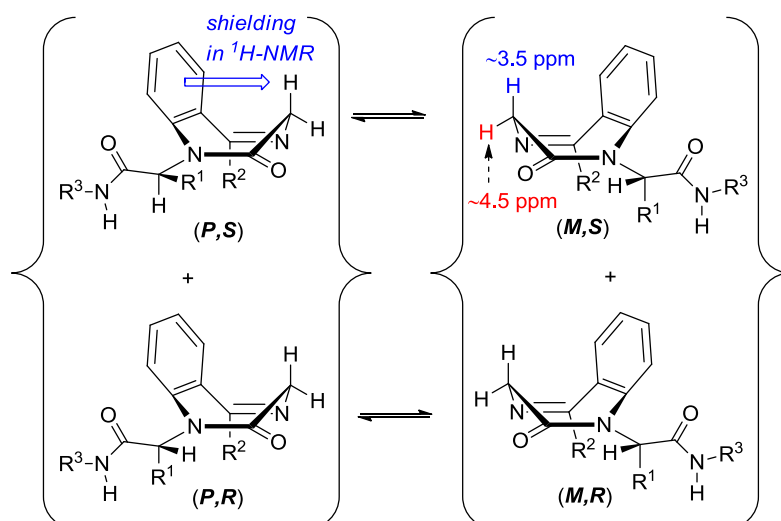
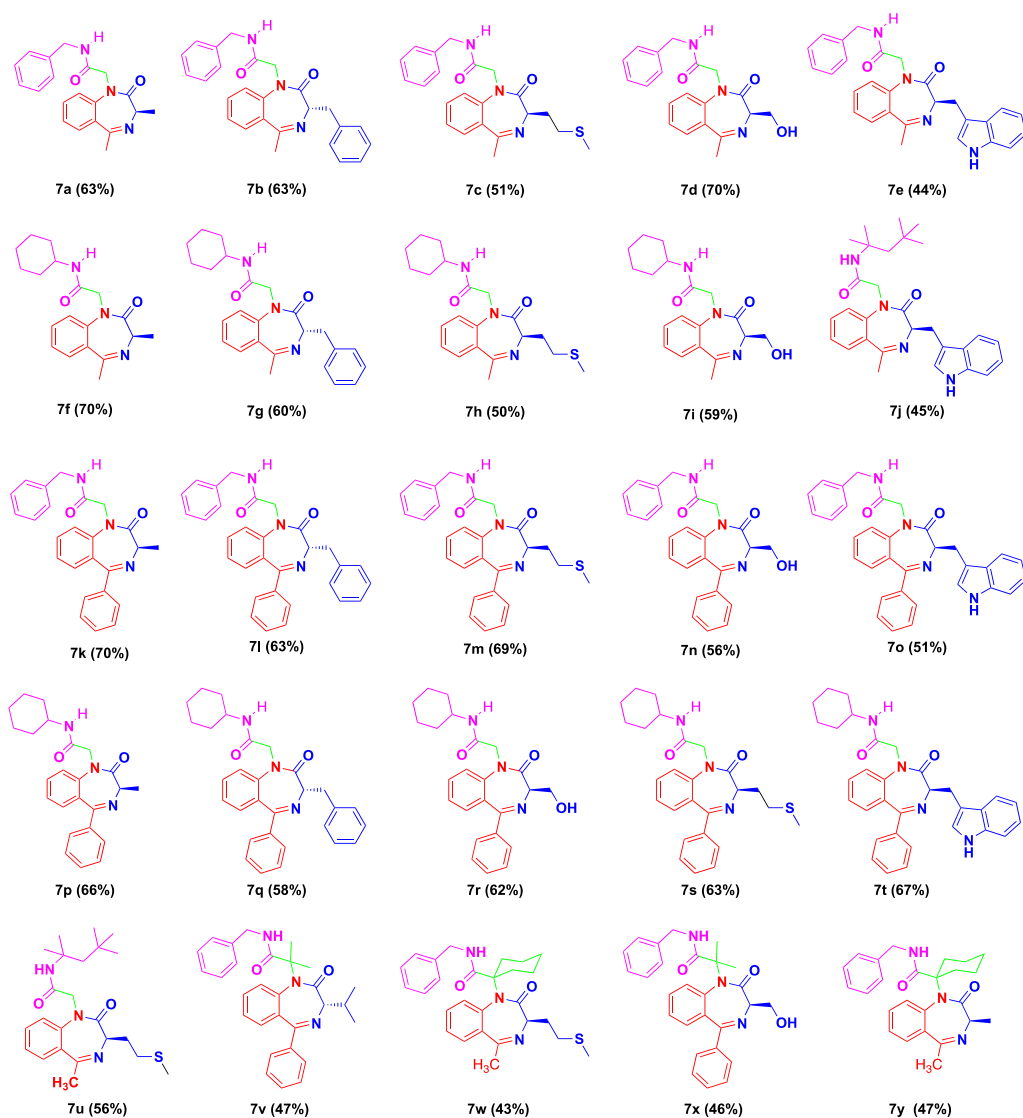
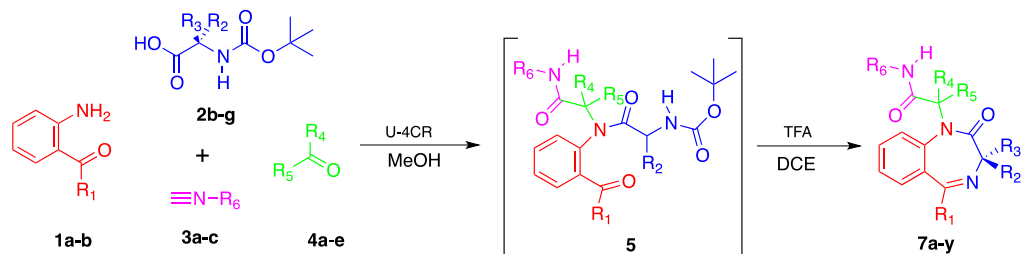


**Figure 4.** Diastereomeric 1,4-benzodiazepin-2-one chemotypes assembled.

Once the feasibility of the proposed method was established for glycine Boc (Scheme 2), and having identified optimal experimental conditions to perform the Ugi–deprotect–cyclize (UDC) sequence, the robustness and scope of the developed methodology was assessed substituting glycine-Boc (**2a**) by a set of assorted protected aminoacids (**2b-g**) as key reactive precursors (Scheme 3). The study capitalizes the excellent commercial availability of enantiopure Boc protected aminoacids (**2**) to introduce functional and stereochemical diversity at position 3 of the heterocyclic framework. Firstly we focused on the generation of collections of BZDs bearing a stereocenter at C3 (Compounds **7**, Scheme 3). With this aim amines **1a-b**, assorted isocyanides (**3**) and either formaldehyde (**4a**) or a symmetric ketone (**4d-e**) were combined in the Ugi reaction with a set of structural and stereochemically diverse enantiopure Boc-protected aminoacids (**2b-g**). We were pleased to observe that only slight modifications of the previously optimized experimental protocol (Scheme 3) were required to verify the transformation of reactive partners of the U-4CR in the  $\alpha$  acylamino amides **5**. A slight excess (1.3 equivalents) of the amine input (**1**) and longer reaction times (48-72 h) were usually required to achieve superior conversion ratios of

the U-4CR, while maintaining mild experimental conditions.

**Scheme 3.** U-4CR-based assembly of enantiopure BZDs incorporating functional and stereochemically diverse groups at position 3.



As for the model systems, smooth cleavage of the protecting group on the Ugi adducts (**5**) employing TFA (DCE/60°C) afforded BZDs **7** in satisfactory yields (44-71%). It was verified that during the synthesis no occurs racemization at the stereocenter ( $ee > 95\%$ ), as determined by chiral-stationary HPLC analysis. A rapid inspection of scheme 3 provides a preliminary assessment of reaction's scope, which generates 1,4-benzodiazepin-2-one collections incorporating 4 points of diversity. As observed, it encompasses use of aliphatic as well as aromatic inputs of all variable components, being not influenced by the electronic and steric variations of the reacting substrates. Significant structural and stereochemical diversity is successfully provided by the aminoacid partner (**2**), as exemplified by a range of diverse residues (including proteinogenic or synthetic aminoacids); some of them bearing challenging residues (e.g. compounds **7i** and **7j**). The NMR data of this series reveals that, for steric reasons, the substituent at C3 is placed preferentially at the pseudoequatorial position (Figure 5). Hence, the 3S and 3R enantiomers will be locked in the M and P conformations respectively and indeed, the  $^1\text{H-NMR}$  of all compounds **7** showed the resonances of a single diastereoisomer, with the H3 resonance around 3.5 ppm, that is a clear indication of its pseudoaxial position. Since a single set of signals is observed in the  $^1\text{H-NMR}$  spectrum, it means that the single enantiomers (M,3S) and (P,3R) were obtained when the (S)- and (R)-aminoacids were respectively used.

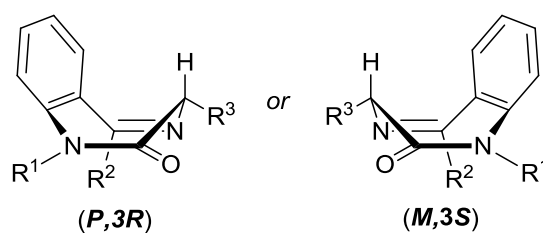


**Figure 5.** Preferred conformations of (P,3R) and (M,3S) enantiomers of 3-substituted benzodiazepines.

The structural assignment within the series (see supporting information) was complemented by X-ray crystallography data obtained on monocrystals of two representative compounds (Compound **7p** and **7u**, Figure 6).<sup>17</sup>

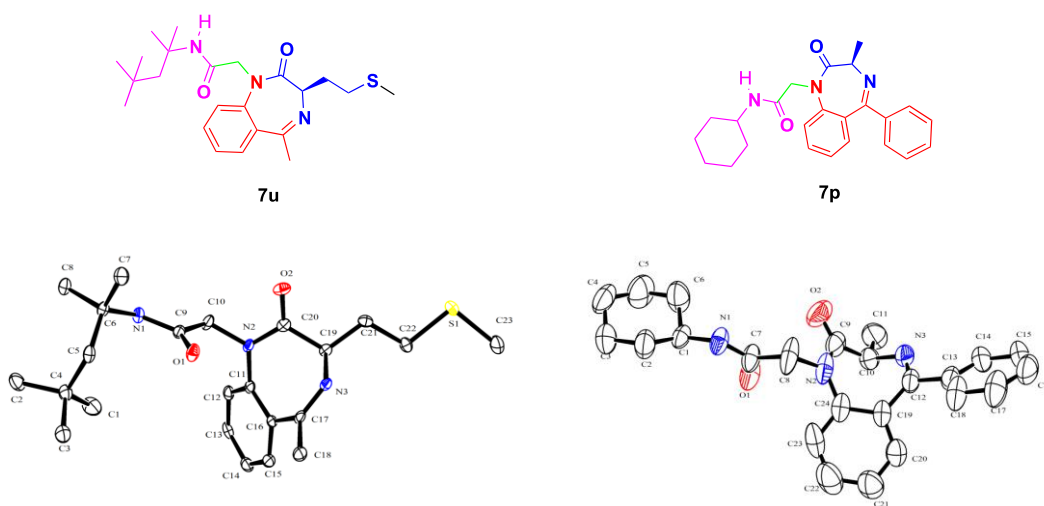
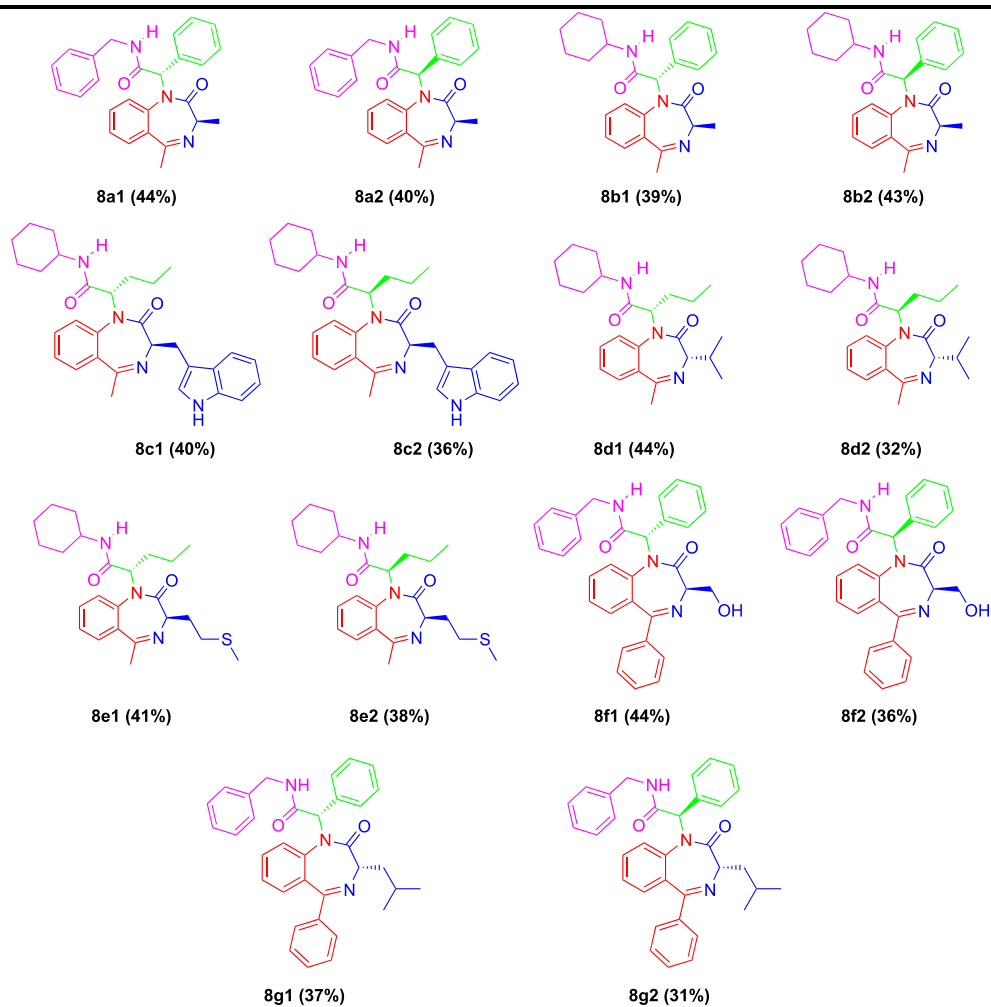
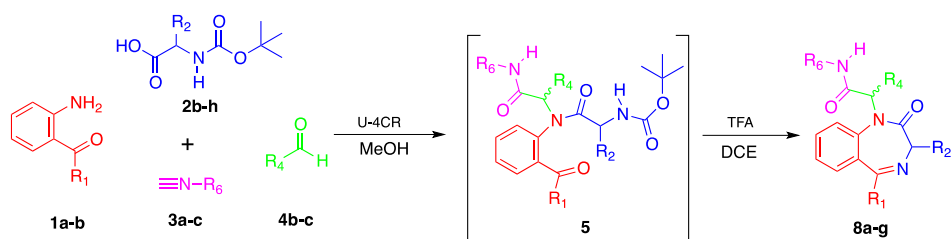


**Figure 6.** Ortep plot showing the crystal structure and atomic numbering scheme for compounds **7p** and **7u**.

The success achieved on previous series led us to evaluate the utilization of prochiral carbonyl components (**4b-c**), which will engender the exocyclic stereocenter formed during the U-4CR (Scheme 4). Butyraldehyde (**4b**) and benzaldehyde (**4c**) were employed in combination with enantiopure N-Boc protected aminoacids (**2b-g**) and the other reactive partners (Scheme 4). These substrates were submitted to stirring at room temperature in methanol affording the corresponding diastereomeric Ugi adducts (**5**) that were directly transformed into BZDs **8** following the Boc-cleavage-cyclization sequence induced by TFA (Scheme 4). The obtained compounds were purified (by either recrystallization or chromatography) and characterized by spectroscopic and analytical techniques; thus verifying the isolation of desired BZDs (**8**) as 1:1 diastereomeric mixtures. Gratifyingly, the exhaustive scrutiny of solvent mixtures enabled to separate a

set of representative diastereoisomers pairs (**8a-g**), employing conventional chromatographic methods. Comparative chiral HPLC analysis of pure samples of the diastereomeric mixture and the optically pure diastereoisomers unequivocally confirmed the optical purity of both pairs.

**Scheme 4. Ugi–Based Assembly of diastereoisomeric BZDs **8****



Due to the difficulties to assign the configuration of the BZDs of the series **8**, and taking into account that important changes in chemical shifts were observed between the diastereoisomeric pairs, we decided to resort to DFT computations as a procedure for the assignment of the relative configurations of the obtained diastereoisomers **8**. In the last decade DFT ab initio chemical shift computations<sup>18</sup> have gradually gained importance among the toolbox used by organic chemists for configurational and conformational analysis through NMR in solution. These studies can be carried out at very affordable computer times, and with enough accuracy, can be successfully employed to distinguish diastereoisomeric structures; even in the presence of conformational flexibility.<sup>19</sup> In the case of flexible molecules, like the ones treated herein, the determination of the configuration is commonly coupled to the determination of the preferred conformational state. We have therefore explored the conformational space of four representative stereoisomers (**8b1**, **8b2** and **8d1**, **8d2**) by means of molecular mechanics Monte Carlo calculations. The obtained molecular mechanics structures were refined at the DFT RI-OPBE level (See experimental section for detailed computational procedures). In accordance with NMR observations the BZD ring is conformationally locked into the boat conformation where the alkyl group at C3 is placed into the equatorial position. Computations show that the conformation of the N1-side chain is dictated by the formation of an intramolecular hydrogen bond between the azepine carbonyl group at C2 and the NH group, which build a new seven membered ring. The two rings adopt a convex-concave disposition as the lowest energy form. Thus, the basal conformation for the (3S,10R) isomer corresponds to a pseudo-axial disposition of the side-chain phenyl group, but a pseudo-equatorial disposition in the case of the (3S,10S) form (Figure 7). The presence of an intramolecular hydrogen bond between the NH and carbonyl C2 was confirmed experimentally by variable temperature <sup>1</sup>H-NMR in CDCl<sub>3</sub> solution, that



yielded temperature coefficients of  $-1.4$  ppb/K for compounds **8d1** and **8d2**. Typically, values more positive than  $-4.5$  ppb/K are considered to support intramolecular H bond.<sup>20</sup>

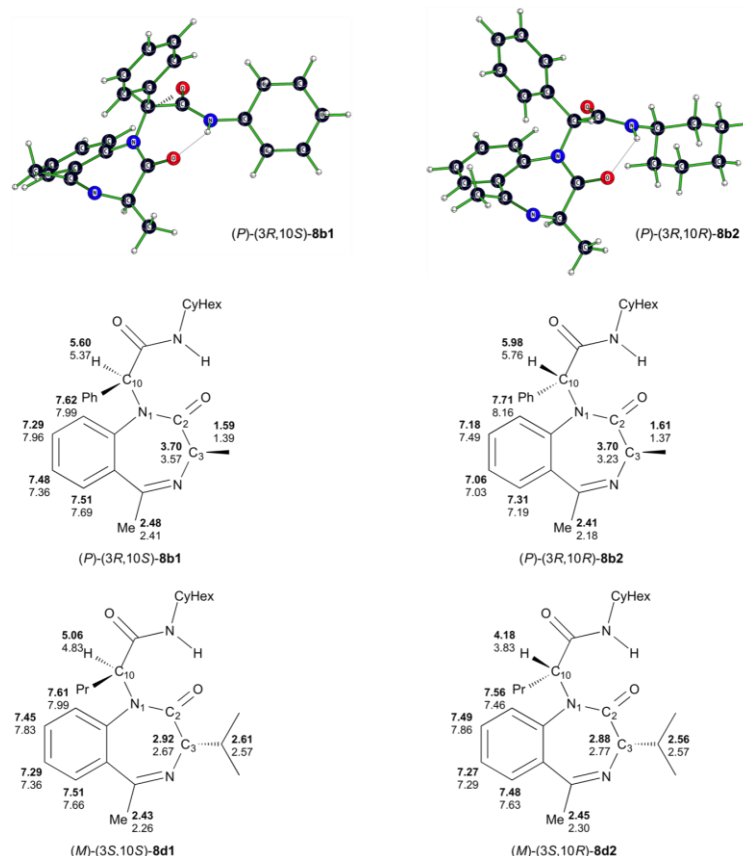


**Figure 7.** Top: DFT lowest energy conformations for  $(P,3R,10S)$ -**8b1** and  $(P,3S,10R)$ -**8b2**. Bottom: Selected experimental (**bold**) vs. computed  $^1\text{H}$  chemical shifts of compounds **8b** (middle) and **8d** (bottom).

$^1\text{H}$  Chemical shieldings were computed at the DFT/IGLO OPBE/pcS-1 level for the lowest energy DFT optimized conformation of each diastereoisomer. The computed shieldings were transformed into chemical shifts by computing shieldings for the tetramethylsilane molecule at the same level of theory. The most remarkable difference between the diastereoisomers is a strong change of the H10 resonance ( $\Delta\delta = 0.38$  ppm and 0.88 ppm in **8b** and **8d**, respectively) in the  $^1\text{H}$  NMR spectra. This agrees with the

DFT computations, that predicted deshielding values  $\Delta\delta = 0.39$  ppm for (*P*,3*R*10*S*)-**8b1** vs (*P*,3*R*10*R*)-**8b2**, and  $\Delta\delta=1.00$  ppm for (*M*,3*S*10*R*)-**8d2** vs. (*M*,3*S*10*S*)-**8d1**. The NMR structural assignment within the series was corroborated by X-ray crystallography data obtained on a monocrystal of the diastereoisomer **8d2** (Figure 7).<sup>21</sup> Note that in the crystal the intramolecular hydrogen bond is no longer present and intermolecular H-bond contacts appear instead. As previously mentioned, the substituent at C3 is preferentially located on the pseudoequatorial position, fixing the BZD core either at the (*M*,3*S*) or at the (*P*,3*R*) conformation. The isopropyl group adopts an antiperiplanar conformation around the H–C–C–H torsion angle. This is also the case in solution as evidenced by a vicinal coupling between H3 and the isopropyl methine proton of ~10 Hz in both isomers **8d1** and **8d2**.

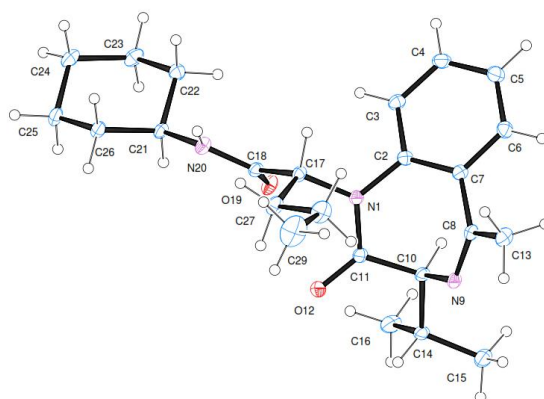


**Figure 7.** Ortep plot showing the crystal structure and atomic numbering scheme for compound **8d2**

As significant differences in the deshielding of the H10 resonance is a common feature of all herein synthesized diastereomeric pairs, we used this diagnostic signal to assign the configuration at C10 for compounds **8**. Supported by the DFT calculations performed (for **8b1**, **8b2**, **8d1**, **8d2**), as well as by the X-ray diffraction analysis of **8d2**, we assumed that the signal for H10 is more deshielded for (*P*,3*R*,10*R*) or (*M*,3*S*,10*S*)

compound than for the corresponding (*P*,3*R*,10*S*) or (*M*,3*S*,10*R*) diastereoisomer. The assignment of the relative configuration at C10 of compounds **8** is presented in Table 1.

**Table 1:** Assignment of C10 configuration on compounds **8** based on chemical shifts of H10.

| <b><math>\delta</math> H10 in ppm / (Configuration)</b>                   |   |
|---|---|
| <i>Diastereoisomer 1</i>  | <i>Diastereoisomer 2</i>  |
| 5.68 / ( <i>P</i> ,3 <i>R</i> ,10 <i>S</i> )- <b>8a1</b>                  | 6.12 / ( <i>P</i> ,3 <i>R</i> ,10 <i>R</i> )- <b>8a2</b>                |
| 5.58 / ( <i>P</i> ,3 <i>R</i> ,10 <i>S</i> )- <b>8b1</b> <sup>a</sup>     | 6.00 / ( <i>P</i> ,3 <i>R</i> ,10 <i>R</i> )- <b>8b2</b> <sup>a</sup>   |
| 4.16 / ( <i>P</i> ,3 <i>R</i> ,10 <i>S</i> )- <b>8c1</b>                  | 5.09 / ( <i>P</i> ,3 <i>R</i> ,10 <i>R</i> )- <b>8c2</b>                |
| 5.05 / ( <i>M</i> ,3 <i>S</i> ,10 <i>S</i> )- <b>8d1</b> <sup>a</sup>     | 4.17 / ( <i>M</i> ,3 <i>S</i> ,10 <i>R</i> )- <b>8d2</b> <sup>a,b</sup> |
| 4.18 / ( <i>P</i> ,3 <i>R</i> ,10 <i>S</i> )- <b>8e1</b>                  | 4.99 / ( <i>P</i> ,3 <i>R</i> ,10 <i>R</i> )- <b>8e2</b>                |
| 5.80 / ( <i>P</i> ,3 <i>R</i> ,10 <i>S</i> )- <b>8f1</b>                  | 6.16 / ( <i>P</i> ,3 <i>R</i> ,10 <i>R</i> )- <b>8f2</b>                |
| 6.27 / ( <i>M</i> ,3 <i>S</i> ,10 <i>S</i> )- <b>8g1</b>                  | 5.79 / ( <i>M</i> ,3 <i>S</i> ,10 <i>R</i> )- <b>8g2</b>                |
| <sup>a</sup> Predicted by DFT calculations. <sup>b</sup> Confirmed by DRX |   |

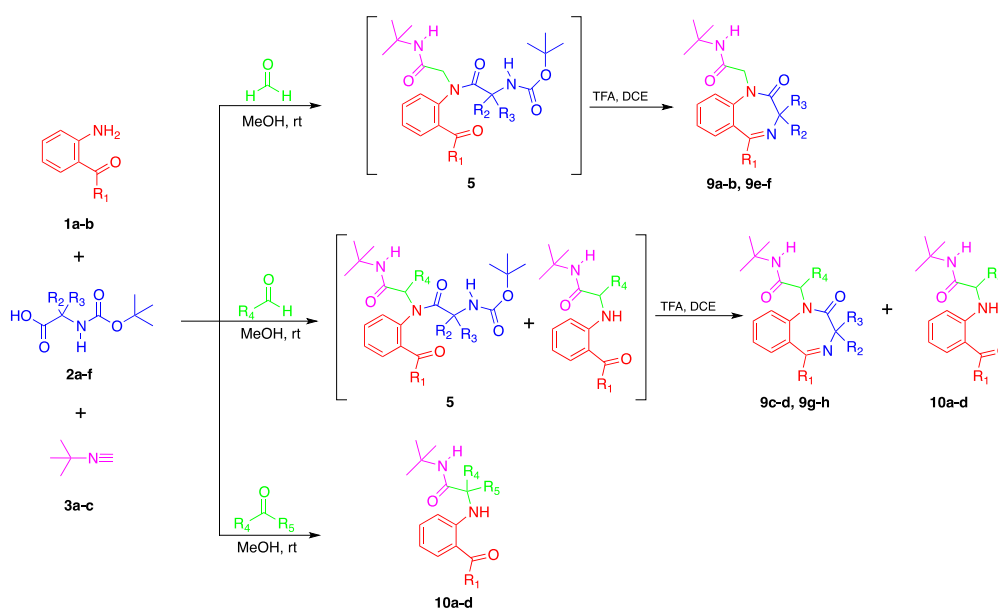
To further challenge the robustness and versatility of the herein documented U-4CR-based strategy, the assembly of BZDs exhibiting challenging substitution patterns at position 3 of the heterocyclic backbone was briefly explored (Scheme 5). It should be noted that, although large and diverse BZD libraries are available; 1,4-benzodiazepin-2-ones featuring quaternary centres at position 3, and particularly spiranic compounds derived of this heterocyclic core, have been only rarely described.<sup>5,6</sup> To the best of our knowledge, there are not precedents of 1,4-Benzodiazepin-2-ones featuring the substitution patterns herein documented (e.g. 3,3-disubstituted and functionalized at position 1, compounds **9**); with its close analogues requiring lineal multistep synthetic strategies that require harsh experimental conditions not compatible with functionalized frameworks.<sup>5,6</sup> Since the introduction of these substitution patterns is expected to profoundly modify the structural features of the heterocyclic core, and accordingly its pharmacological profile, novel methods providing a rapid and experimentally simple

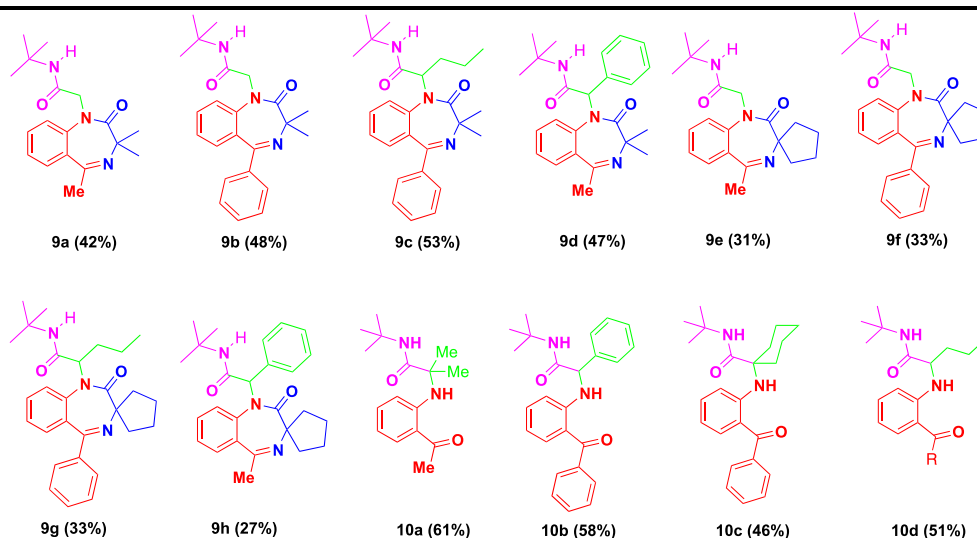
entry to these chemotypes remains a highly pursued methodological challenge.

Two sterically hindering N-Boc protected carboxylic acids [e.g. 2-((*tert*-butoxycarbonyl)amino)-2-methylpropanoic acid (**2i**) and 1-((*tert*-butoxycarbonyl)amino)cyclopentanecarboxylic acid (**2j**)] were selected as model substrates to study the proposed U-4CR sequence (Scheme 5); in combination with the precursors employed along this study [e.g. amines **1a-b**, tertbutyl isocyanide (**3c**) and the four carbonyl components (**4a-d**)]. The information contained in scheme 5 reveals novel reactivity facets of herein described Ugi-based BZDs assembly, while exemplify its contribution in terms of rapid access to complex and hitherto unexplored diversity spaces. The preliminary screening of the transformation revealed a significant decreasing on the reactivity profile and scope respect previous series (Schemes 2-4), with reaction behaviour being highly dependent of the starting carbonyl compound (Scheme 5). Thus, aldehydes evaluated (formaldehyde, butyraldehyde and benzaldehyde) smoothly underwent the U-4CR, albeit with a reduced efficiency respect previous series, affording the corresponding Ugi adducts that were subsequently cyclized (Scheme5). It should be noted that isolated yields of BZDs **9** range from satisfactory to moderate (35-52%), clearly correlating with the steric hindering within the starting aldehyde (Scheme 5). In a clear contrast, the U-4CR employing ketones (propanone and cyclohexanone) failed to provide the desired Ugi adducts (Scheme 5); exclusively affording keto aminoacetamides **10** (43-66%) and variable amounts of the unreacted precursors. All attempts to improve these results, by varying reagents ratio, solvents (EtOH, CF<sub>3</sub>CH<sub>2</sub>OH, toluene, DCM) temperatures (45, 60°C) did not modify reaction outcome; at either the qualitative (compound isolated) or quantitative (yield) level. With the exception of U-4CR that employ formaldehyde as carbonyl component, all

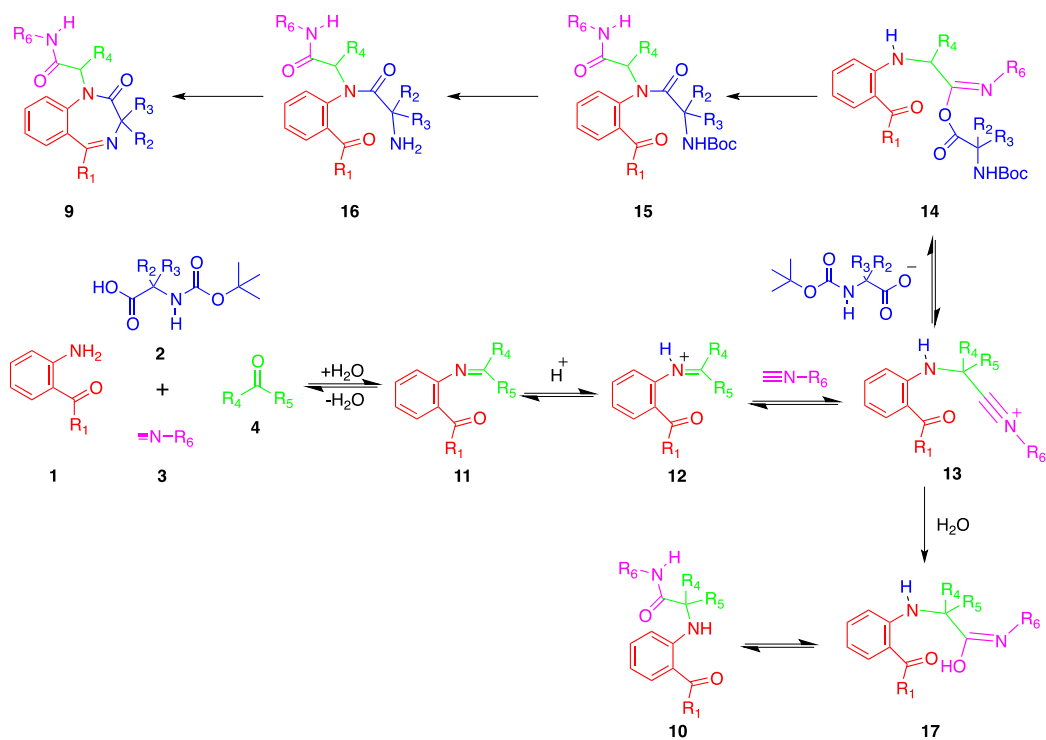
transformations employing **2i** and **2j** afforded variable amounts of substituted keto aminoacetamides **10**; which becomes the only isolated reaction product when employing ketones. Such an experimental outcome, not observed for the less congested aminoacids (Schemes 2-5), clearly reflects the impossibility of the substituted carboxylic acid (carboxylate to be more precise) to attack steric hindering nitrilium ion intermediates. It should be noted that, although the steric factors showed to exert a key role on reaction behaviour, the substituent present in the starting amine ( $R_1 = \text{Me}$  or  $\text{Ph}$ ) seems do not affect reaction's viability (Scheme 5).

**Scheme 5.** Ugi–Based Assembly of 1,4-benzodiazepin-2-ones featuring quaternary centres at C3.





Although it is premature to propose a detailed mechanism at this stage; a plausible mechanistic proposal, consistent with the above-described experimental results, is presented in Scheme 6. The overall transformation would start with imine formation (**11**) and its subsequent protonation, thus generating the iminium ion **12**; which rapidly undergoes nucleophilic addition of the isocyanide to generate the highly reactive nitrilium **13**. At this point of the transformation the steric hindering on the nitrilium ion intermediate (**13**) govern the reaction outcome. Thus, less congested nitrilium adducts ( $R_4 = R_5 = H$ ) follow the normal course of the U-4CR [e.g. carboxylate insertion to give **14** and then Mum rearrangement] affording the expected Ugi adducts (**15**), that upon acid-mediated cleavage generate the targeted BZDs (**9**). In contrast, for nitrilium ions **13** derived of butyraldehyde, benzaldehyde or ketones the reaction behaviour heavily depends of its substitution pattern at the acetamide linkage. The superior steric hindering in these intermediates partially, or completely (for those derived of ketones), prevents the nucleophilic addition of the carboxylate ion; accordingly a water molecule could intercept the reactive nitrilium intermediate (**17**) to afford the isolated keto aminoacetamides **10**.



**Scheme 6.** Mechanistic proposal for the Ugi-Based Assembly of 3,3-substituted 1,4-benzodiazepin-2-ones

In summary, we have documented a convergent approach that enables the straightforward assembly of 1,4-benzodiazepin-2-ones exhibiting high skeletal, functional and stereochemical diversity. This versatile integrated U-4CR-based strategy, that exhibits high bond-forming efficiency as well as structure and step economies, not requires advanced intermediates, anhydrous solvents or transition metal catalysts; thus exemplifying the reconciliation of molecular complexity and functional diversity with experimental simplicity. Further work is in progress in our laboratories to apply this method to the synthesis of novel BZD derivatives and complete the pharmacological evaluation of herein documented library.

## Experimental Section

Commercially available starting materials and reagents were purchased and used without further purification from freshly opened containers. All solvents were purified and dried by standard methods. Organic extracts were dried with anhydrous sodium sulphate. The reactions were monitored by TLC and purified compounds each showed a single spot. Unless stated otherwise, UV light and/or iodine vapour were used for the detection of compounds. The synthesis and purification of all compounds were accomplished using the equipment routinely available in organic chemistry laboratories. Most of the preparative experiments were performed in coated vials on an organic synthesiser with orbital stirring. Purification of isolated products was carried out by recrystallization or chromatographic methods. Reported yields correspond to the mean of two synthetic experiments. Compounds were routinely characterised by spectroscopic and analytical methods. Melting points were determined on a melting point apparatus and are uncorrected. The chemical structures of the obtained compounds were characterized by nuclear magnetic resonance spectroscopy ( $^1\text{H}$  and  $^{13}\text{C}$ ) and high-resolution mass spectra (HRMS). Unless otherwise quoted, NMR spectra were recorded in  $\text{CDCl}_3$ . Chemical shifts are given as  $\delta$  values against tetramethylsilane as internal standard and  $J$  values are given in Hz. All NMR experiments were carried out at 298 K on a Bruker Avance 600 spectrometer operating at 600.13 MHz for  $^1\text{H}$ , 150.90 MHz for  $^{13}\text{C}$  and 90.56 MHz for  $^2\text{H}$ , equipped with a triple resonance inverse (TXI) room temperature probe with Z-only gradients.  $^1\text{H}$  and  $^{13}\text{C}$  resonances of (SR)602 and (SS)-602 in  $\text{CDCl}_3$  solutions were assigned from ge-HSQC, ge-HMBC and ge-COSY experiments. Shifts were referenced to the corresponding  $\text{CCl}_3$  (7.26) and  $\text{CDCl}_3$  peaks (77.0) ppm. The enantiomeric (or diastereomeric) excesses were determined by chiral-stationary phase HPLC employing variable mixtures of *n*-hexane-isopropanol.



The conformational spaces of the diastereoisomers were explored using the Monte Carlo torsional procedure as implemented in the Macromodel 9.1 software package using the MMFF94 force field. The lowest MMFF94 energy structures were refined at the RI<sup>22</sup>-DFT BP86 level using the defbas-1 basis set<sup>23</sup> (QuickOpt option in ORCA package) and the def2-TZV auxiliary basis set.<sup>24</sup> Chemical shifts were computed at the IGLO<sup>25</sup> RI-OPBE<sup>26</sup>/pcS-1<sup>27</sup> level for the lowest energy DFT optimized conformation of each diastereoisomer. The SV/J auxiliary basis set was employed for density fitting. Solvation was taken into account using the COSMO model.<sup>28</sup> The computed shieldings were transformed into chemical shifts by computing shieldings for the tetramethylsilane and benzene molecules at the same level of theory. The benzazepine aromatic protons were reference according to benzene shielding whereas the rest of protons were reference to TMS. The shifts were computed according to the relationship:

$$d_{calc} = \frac{S_{ref} - S_{calc}}{1 - S_{ref}}$$

where  $\sigma_{ref}$  and  $\sigma_{calc}$  are the shieldings computed for the reference proton nuclei and the proton of interest in the benzodiazepine. All computations were performed using the Orca 2.9 software package.<sup>29</sup>

#### **General procedure for the one-pot synthesis of 1,4-benzodiazepin-2-ones 6-**

**9.** A mixture of the carbonyl compound (1.0 mmol), the amine (1.3 mmol), the isocyanide (1.0 mmol) and the protected aminoacid (1.0 mmol) in MeOH (3 mL) was submitted to orbital stirring at room temperature for 48–72 h. After completion of the reaction, CH<sub>2</sub>Cl<sub>2</sub> (3 mL) and PS-*p*-TsOH (2.0 mmol) were added. The reaction mixture was submitted to orbital stirring at room temperature until complete consumption of the unreacted isocyanide (30–60 min). The polymeric reagent was filtered off and

successively washed [2 times (4 mL)] with MeOH, AcOEt and CH<sub>2</sub>Cl<sub>2</sub>. Evaporation of the solvents from the filtrate afforded a residue, which was treated with 20% TFA in DCE (and heated to 60°C for 1h). The obtained solution was then treated with saturated NaHCO<sub>3</sub>. After extraction with ethyl acetate, the organic phase was dried (Na<sub>2</sub>SO<sub>4</sub>) and evaporated under reduced pressure to afford an oily residue that was purified by chromatographic methods on silica gel using hexane/AcOEt mixtures.

**Acknowledgements.** This work was financially supported by the Fondo Europeo de Desarrollo Social (FEDER) and the Galician Government (Spain), Project: 09CSA016234PR. J.A. thanks FUNDAYACUCHO (Venezuela) for a predoctoral grant and Deputación da Coruña (Spain) for a post-doctoral research grant. ANV thanks Spanish government for a Ramón y Cajal research contract.

**Supporting Information Available.** Detailed experimental procedures, spectroscopic data and copies of NMR and mass spectra for representative compounds described. This information is available free of charge via the Internet.

## References and Notes

- (1) Kleemann, A., Engel, J., Kutscher, B., Reichert, D., *Pharmaceutical Substances: Synthesis, Patents, Applications*, 5th ed., Thieme: Stuttgart, 2008.
- (2) Evans, B. E., Rittle, K. E., Bock, M. G., DiPardo, R. M., Freidinger, R. M., Whitter, W. L., Lundell, G. F., Veber, D. F., Anderson, P. S., Chang, R. S. L., Lotti, V. J., Cerino, D. J., Chen, T. B., Kling, P. J., Kunkel, K. A., Springer, J. P., Hirshfield, J., *J. Med. Chem.*, **1988**, *31*, 2235–2246.

- (3) Bateson, A. N., *Sleep Med.*, **2004**, suppl, 1, S9–S15.
- (4) Bolli, M. H., Marfurt, J., Grisostomi, C., *J. Med. Chem.* **2004**, *47*, 2776–2795. De Clerq, E., *Antiviral Res.* **1998**, *38*, 153–179. Doulat, J., Liu, W., Gresh, N., Garbay, C., *Biorg. Med. Chem. Lett.*, **2007**, *17*, 2527–2530. Ettari, R., Micale, N., Schirmeister, T., Gelhaus, C., Leippe, M., Nizi, E., Di Francesco, M. E., Grasso, S., Zappalà. *J. Med. Chem.*, **2009**, *52*, 2157–2160. Micale, N., Vairagoundar, R., Yakovlev, A. G., Kozikowski, A. P., *J. Med. Chem.*, **2004**, *47*, 6455–6458.
- (5) The helical descriptors (*M*)- and (*P*)- are based on the sign of the  $\tau_{2345}$  torsional angle. For recent studies on this conformational inversion, see: Hsu, D. C.; Lam, P. C.-H.; Slebodnick, C.; Carlier, P. R. *J. Am. Chem. Soc.* **2009**, *131*, 18168–18176. Carlier, P. R.; Sun, Y. S.; Hsu, D. C.; Chen, Q. H. *J. Org. Chem.* **2010**, *75*, 6588–6594.
- (6) Linscheid P, Lehn J-M. E., *Bull. Soc. Chim. Fr.*, **1967**; 992–997. Carlier, P. R., Zhao, H., Mac-Quarrie-Hunter, S. L., DeGuzman, J. C., Hsu, D. C., *J. Am. Chem. Soc.* **2006**, *128*, 15215–15220.
- (7) Gilman, N. G., Rosen, P., Earley, J. V., Cook, C., Todaro, L. J., *J. Am. Chem. Soc.* **1990**, *112*, 3969–3978. Lam, P. C. H., Carlier, P. R., *J. Org. Chem.*, **2005**, *70*, 1530–1538.
- (8) Horton, D. A., Bourne, G. T., Smythe, M. L., *Chem. Rev.*, **2003**, *103*, 893–930.
- (9) Yang, S. K., *Chirality*, **1994**, *6*, 175–184. Atkins, R. J., Banks, A., Bellingham, R. K., Breen, G. F., Carey, J. S., Etridge, S. K., Hayes, J. F., Hussain, N., Morgan, D. O., Oxley, P., Passey, S. C., Walsgrove, T. C., Wells, A. S., *Organic Process Research & Development* **2003**, *7*, 663–675.
- (10) *Multicomponent Reactions*, Zhu, J., Bienayme, H., Ed., Wiley-VCH, Weinheim, **2005**. Dömling, A., *Chem. Rev.* **2006**, *106*, 17–89. Armstrong, R.W., Combs, A. P., Tempest, P. A. Brown, S. D., Keating, T. A., *Acc. Chem. Res.* **1996**, *29*, 123–131.

- (11) For representative examples see: Shaabani, A., Rezayan, A. H., Keshipour, S., Sarvary, A., Ng, S. W., *Org. Lett.*, **2009**, *11*, 3342–3345. Guggenheim, K. G., Toru, H., Kurt, M. J., *Org. Lett.*, **2012**, *14*, 3732–3735. Donald, J. R., Wood, R. R., Martin, S. F., *ACS Comb. Sci.*, **2012**, *14*, 135–143. Xu, J., Bian, L., Zhang, J., Chen, J., Deng, H., Wu, X., Zhang, H., Cao, W., *Chem. Commun.*, **2011**, *47*, 3607–3609.
- (12) For representative examples see: Keating, T. A., Armstrong, *J. Org. Chem.*, **1996**, *61*, 8935–8939. De Silva, R. A., Santra, S., Andreana, P. R., *Org. Lett.*, **2008**, *10*, 4541–4544. Marcaccini, S., Miliciani, M., Pepino, R., *Tetrahedron Lett.*, **2005**, *46*, 711–713. Tempest, P., Pettus, L., Gore, V., Hulme, C., *Tetrahedron Lett.*, **2003**, *44*, 1947–1950. Shaabani, A., Rezayan, A. H., Keshipour, S., Sarvary, A., Weng, S., *Org. Lett.*, **2009**, *11*, 3342–3345. Cuny, G., Bois-Choussy, M., Zhu, J., *J. Am. Chem. Soc.*, **2004**, *126*, 14475–14484. Sañudo, M., García-Valverde, M., Marcaccini, S., Delgado J. J., Rojo, J., Torroba, T., *J. Org. Chem.*, **2009**, *74*, 2189–2192.
- (13) Gordon, C. P., Young, K. A., Hizartzidis, L., Deane, F. M., McCluskey, A., *Org. Biomol. Chem.*, **2011**, *9*, 1419–1428. He, P., Nie, Y., Wu, J., Ding, M. W., *Org. Biomol. Chem.*, **2011**, *9*, 1429–1436. Marcaccini, S., Pepino, R., Pozo, M. C., Basurto, S., García-Valverde, M., Torroba, T., *Tetrahedron Lett.*, **2004**, *45*, 3999–4001.
- (14) Lecinska, P., Corres, N., Moreno, D., García-Valverde, M., Marcaccini, S., Torroba, T., *Tetrahedron*, **2010**, *66*, 6783–6788.
- (15) Huang, Y., Khoury, K., Chanas, T., Dömling, A., *Org. Lett.*, **2012**, *14*, 5916–5919.
- (16) Azuaje, A., Coelho, A., El Maatougui, A., Blanco, J. M., Sotelo, E., *ACS Comb. Sci.*, **2011**, *13*, 89–95.
- (17) The Supporting Information contains the crystallographic information files (CIF)

- of compounds **7p** and **7u**. Additional information can be obtained free of charge from The Cambridge Crystallographic Data Centre (CCDC 915940 and CCDC 915941).
- (18) Lodewyk, M. W., Siebert, M. R., Tantillo, D. J., *Chem. Rev.*, **2012**, *112*, 1839–1862. Petrovich, A., Navarro-Vázquez, A., Alonso-Gómez, J. L., *Curr. Org. Chem.*, **2010**, *14*, 1612–1628.
- (19) Smith, S. G., Goodman, J. M., *J. Am. Chem. Soc.*, **2010**, *132*, 12946–12959. Smith, S. G., Goodman, J. M., *J. Org. Chem.*, **2009**, *74*, 4597–4607.
- (20) Belvisi, L., Gennari, C., Mielgo, A., Potenza, D., Scolastico, C., *Eur. J. Org. Chem.* **1999**, *1999*, 389–400.
- (21) The Supporting Information contains the crystallographic information files (CIF) of compound **8d2**. Additional information can be obtained free of charge from The Cambridge Crystallographic Data Centre (CCDC 915942).
- (22) (a) Baerends, E.J., Ellis, D. E., Ros., P., *Chem. Phys.*, **1973**, *2*, 41–51. (b) K. Eichkorn, K., Weigend, F., Treutler, O., Ahlrichs., R., *Theor. Chem. Acc.*, **1997**, *97*, 119–124.
- (23) Schaefer, A., Horn, H., Ahlrichs. R., *J. Chem. Phys.* **1992**, *97*, 2571–2577.
- (24) Weigend, F., Ahlrichs, R., *Phys. Chem. Chem. Phys.* **2005**, *7*, 3297–3305.
- (25) Kutzelnigg, W., Fleischer, U., Schindler. M. The IGLO-Method: Ab Initio Calculation and Interpretation of NMR Chemical Shifts and Magnetic Susceptibilities, volume 23. Springer Verlag, 1990.
- (26) Zhang, Y.; Wu, A.; Xu, X.; Yan, *Chem. Phys. Lett.* **2006** *421*, 383–388.
- (27) Jensen, F., *J. Chem. Theory Comput.* **2008**, *4*, 719–727.
- (28) Sinnecker, S.; Rajendran, A.; Klamt, A.; Diedenhofen, M.; Neese, F. *J. Phys. Chem. A* **2006**, *110*, 2235–2245.

(29) Neese, F. *WIREs Comput. Mol. Sci.*, **2012**, *2*, 73–78.